Caving 2022 - Y Potvin (ed.)

doi:10.36487/ACG_repo/2205_69

Empirical damage prediction in sublevel cave crosscuts at the Malmberget mine

TH Jones *LKAB, Sweden*

D Saiang *Luleå University of Technology, Sweden*

Abstract

Building on the empirical research completed in the footwall contact zone of LKAB's Malmberget mine, a method has been developed for predicting damage in the crosscut entries of the mine layout. Three-dimensional stress measurements combined with analyses of measured and observed damage in the crosscuts have allowed new interpretations of the crosscut performance. Stress analysis focused on the relative differential stresses measured in the area of interest. These stress changes were then linked directly to observed changes in the entry condition according to the Entry Condition Rating (ECR) system, a damage mapping system developed for the mine. A bilinear model was used to describe the entry condition rate of change such that the peak measured differential stress corresponds to increased degradation rates. These bilinear degradation rate trends are shown to be directly related to the geotechnical qualities of the rock using the Geologic Strength Index (GSI) of the monitored locations, irrespective of lithology. The final step was to develop an empirical model that allows prediction of a crosscut's future ECR based on changes in the relative differential stress and the GSI of the crosscut. In combination with simple numerical modelling tools the model can be used to predict ahead of time when additional reinforcement will be necessary.

Keywords: *differential stress, damage, condition ratings, Geologic Strength Index*

1 Introduction

Sweden's LKAB mining company was founded in 1890, though mining in the region goes back to 1660s when the first ore sample was collected. Today LKAB operates two underground iron mines, Kiirunavaara and Malmberget, where sublevel caving is the primary mining method. The Malmberget mine comprises some 20 orebodies, of which about half of them are in production today and has an annual production around 18 Mtpa. The mine is in the municipality of Gällivare, Norrbotten county, in northern Sweden. Today's mining is conducted at 800–1,200 m depth, distributed over an area of approximately 2.5 km × 5 km (NS × EW). The dip of the orebodies varies between 15° and 75°, with an average dip of 45°–50°.

Mining is carried out using the sublevel caving method which unavoidably results in redistributions of the stresses moving through the rock. As development progresses, these stresses can concentrate in sensitive areas leading to rockfalls and high deformation. When excavation and extraction proceeds to deeper levels stresses accumulate and can overcome the strength of the rock mass hosting the excavations.

In Malmberget, difficulty is encountered when excavating through geologies with highly varied properties, such as is encountered when sedimentary material is replaced by igneous intrusives or magma bodies. Stresses in these areas are concentrated not only under the effect of multiple different excavations, but by the natural capabilities of the different geologies to withstand and/or transmit that stress. It is an area where rock support can be challenging at best, and nearly impossible at worst. The best designed support systems can still yield to the conditions it is placed under, allowing rock conditions to degrade and underground areas to become less safe. A great deal of effort may be placed in routine inspections, scanning, and instrumentation, yet in a mine as large as Malmberget that has more than 500 km of underground tunnels, routine inspections become impossible. A better way is to focus inspections and pre-emptive reinforcement activities into areas known and expected to worsen, yet to do that one must know where to look.

The safest reinforcement is the reinforcement that is installed before it is needed, though this is not necessarily the most cost-effective. A balance should be found that maximises the stability of the openings while also minimising the amount of unnecessary pre-emptive reinforcement (that reinforcement which ultimately isn't necessary). The first part of this path is being able to identify when underground openings will degrade to the point that reinforcement is necessary. This paper looks at the work done in Malmberget as part of a large research study to better understand how mining-induced stresses and geologically driven stress concentrations interact to induce rock failure, especially in conjunction with rock quality variations (Jones & Saiang 2022a).

Differential stresses have been shown to be closely tied to the failure mechanisms of rocks (Feng et al. 2021). In this paper, empirical analysis uses an Entry Condition Rating (ECR) system (Jones & Saiang 2022b) and in situ differential stress measurements, to develop methods for predicting (potentially in advance of development) entry damage and degradation.

2 Site description

2.1 Geology

The ore in Malmberget is approximately 90% magnetite (MGN) with areas of hematite (HRM) and apatite (APA). The orebody includes a vein system with impregnations of several minerals and is strongly affected by metamorphic recrystallisation. The main gangue minerals are amphibole, pyroxene and biotite and granitic intrusions often cross the ore (Bergman et al. 2001). The thickness of the orebodies ranges between 20 m and 100 m. The volcanic host rock consists of grey (GLE), grey-red (GRL), red-grey (RGL) and red leptites (RLE) with increasing strength (Jones et al. 2019), along with granite (GRA).

A biotite schist (BSF) is also found in the mine occurring in a layered structure along the strike and dip of the orebody footwall contact and is the weakest unit compared to the other rock types in the mine. Its most pure forms tend to occur in direct contact with the ore, though it also exists in veins or inclusions of varying proportions in the other major geological units. The rock mass strength and opening stability in any particular location are generally directly related to the presence of the schist. The different lithologies vary in grain size and mineralogy, but all of them tend have some amount of biotite content included. The higher the rock mass strength, the lower the biotite content.

The geology of the Malmberget mine gives an excellent opportunity to investigate the interplay of stresses flowing through materials of varying geotechnical quality near one another. The best location for this exists along the footwall contact with the orebody. At these locations there is often a zone where the leptite host rock (typically grey or red in the areas under consideration) and the magnetite ore are separated by a thin layer (5–10 m) of biotite schist or grey leptite. These three geologies have very different strength and deformation characteristics. Their dimensions and proximity are such that all three materials can be instrumented in one crosscut and have a situation where it can be reasonably expected that each of the instruments are undergoing the same general stress redistribution process yet may produce different results due to the varied rock properties.

2.2 Mining method

Mining in the study areas is transverse sublevel caving. In this method rings of 8–14 production blastholes are drilled upwards into in a trapezoidal fan pattern in the roof at 3.5 m intervals. The first three rings in each crosscut are spaced closer together to create a larger initial opening designed to begin mining. The rings are long enough to reach through the undisturbed rock above the entry up to the previous sublevel, meaning that the centre holes can be up to 60 m long, while the sides are typically around 30–32 m long. After the crosscut is opened for mining, the remaining blast rings are loaded and detonated one at a time towards the footwall drift. The large size of the blast rings produces a noticeable stress re-distribution throughout the mine area, and it is this stress redistribution that drives much of the damage that occurs in the crosscuts.

Rock support in the area routinely consists of 3.05 m long dynamic bolts with a 1 m × 1 m spacing, 10 cm thick fibre-reinforced shotcrete, and dynamic welded-wire mesh.

The work done in this project extends through the Alliansen (AL), Hoppet (HO) and Printzsköld (PR) orebodies. The Alliansen orebody is furthest east of the three and is one of the oldest orebodies in the mine. It was first mined as an open pit beginning in 1905 and then converted to full-scale sublevel caving below the 300 m level. Level numbers correspond to a local coordinate system where depth and level numbers increase downwards, relative to the top of the mountain. The PR orebody is the furthest west and first began production on level 780, proceeding downwards from there. The two orebodies begin to merge around level 1000, with the HO orebody becoming a distinct entity beginning on level 1023 in-between them. From that depth onwards the three orebodies form a combined ore unit along with the Gunilla (GN) orebody, sitting west of PR. The combined footwall drive for those four orebodies is approximately 2 km long.

3 Instrumentation and data collection

3.1 Instrumentation sites and input data

The premise of the instrumentation plan was that the mining activities redistribute the pre-existing stresses in the area and that these stress redistributions create increased stress magnitudes and concentrations which are channelled through and around the development openings in the mine. Depending on the rock quality parameters and geometries, this can result in stress change, seismicity, and/or deformation. The instrumentation and data collection plan were devised to capture both the driving stress changes and the resulting damage and deformation in the footwall contact zone and its varying geologies.

Instrumentation sites used in this paper were in PR level 1023 crosscut 4080 (PR4080) and AL level 1082 crosscut 2780 (Figures 1 and 2). There were three instrumented profiles installed in each crosscut aligned in such a way that they were in a single geology as much as was possible.

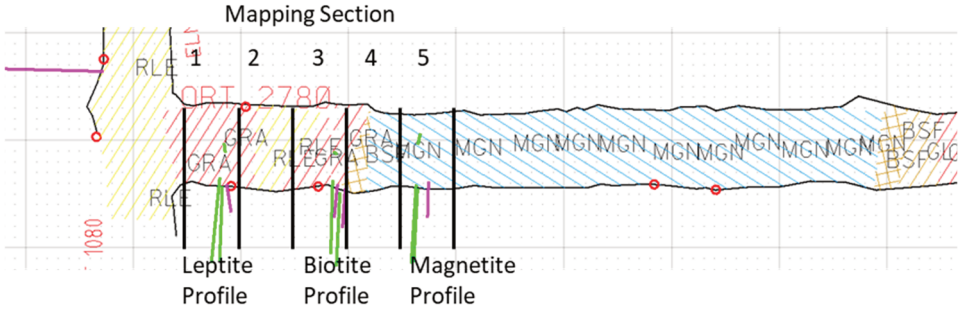

Figure 1 Instrumentation profiles combined with damage mapping sections in a geologic map of the AL2780 instrumentation site. Extensometers installed along green lines and stress cells at the end of pink lines. Grid is 10 × 10 m

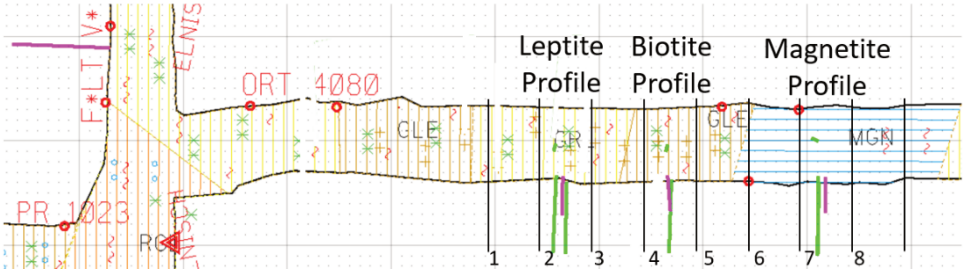

Figure 2 Instrumentation profiles combined with damage mapping sections in a geologic map of the PR4080 instrumentation site. Extensometers installed along green lines and stress cells at the end of pink lines. Grid is 10 × 10 m

The instrument profiles were installed according to the design shown in Figure 3, which shows the lengths and depths of the various instruments and anchors. Anchor positions and stress cells were close to the excavation wall in order to better reflect the stress conditions and in the actual deformation zone. The two sites were located approximately 575 m apart from one another horizontally, and approximately 60 m apart from one another vertically (Figure 4).

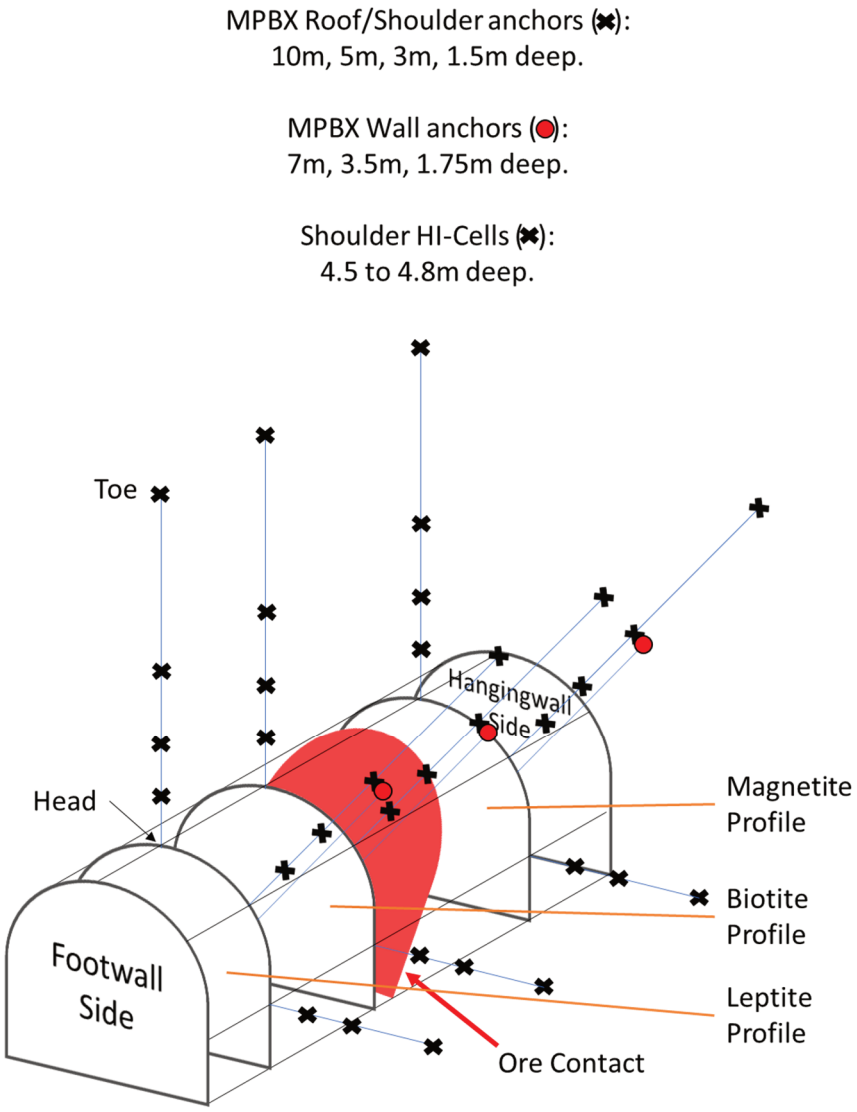

Figure 3 Instrumentation layout including anchor positions and instrument lengths

The total instrumentation and data collection for each site included stress measurements were made with 3D digital hollow inclusion stress cells (HID-cells) which acquired stress data relative to the beginning of the measurement period. Deformation was collected with a combination of multiple-point borehole extensometers, wall-to-wall convergence stations (using a laser distance metre) and floor heave measurements. Entry damage was tracked by establishing 5 m long damage mapping zones throughout the instrumentation areas (Figures 1 and 2). Convergence and floor heave measurements were taken at the start and finish of each damage mapping zone. Additional input data included geologic mapping and Geologic Strength Index (GSI) data collected by the mine geologists for most of the damage profiles. For the work in this paper the primary data sources were the HID-cells and the damage mapping which is covered in greater detail in a companion article (Jones & Saiang 2022b).

Much greater detail can be found in the full report of this project (Jones & Saiang 2022a), but Table 1 shows an overview of the total amount of instrumentation installed in the two crosscuts referenced in this study,

it's accuracy and resolution, as well as the collection time intervals. Much more data from other crosscuts was used to help with interpretation and understanding of the mechanisms at work.

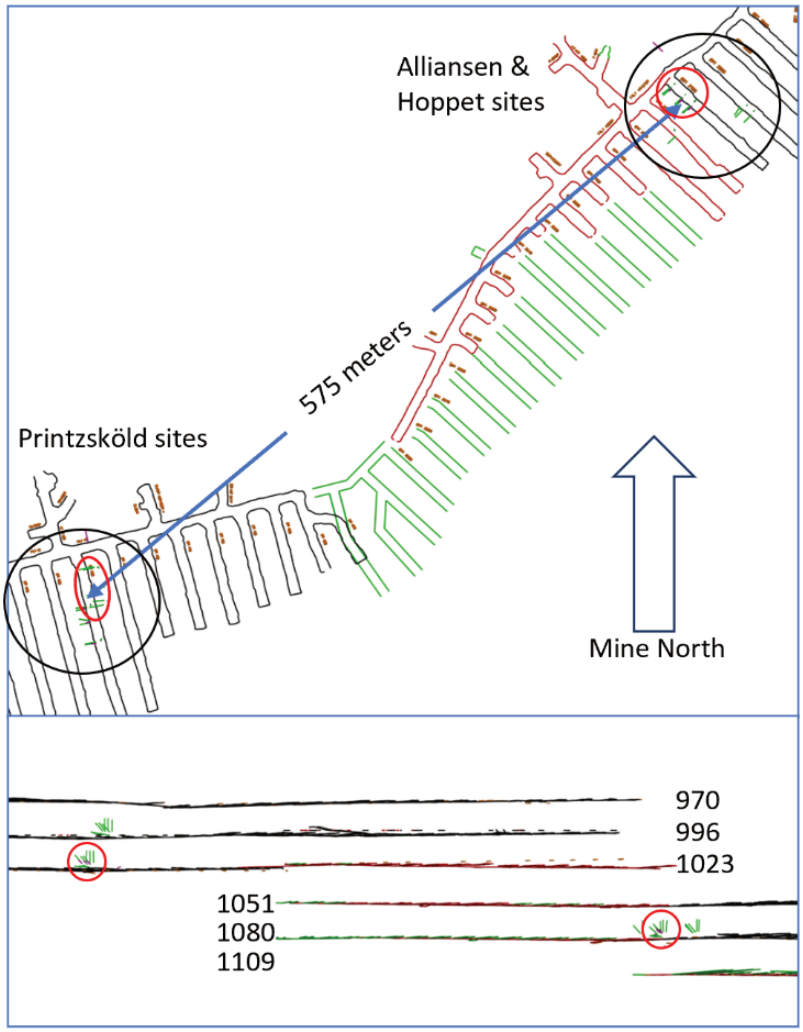

Figure 4 Mine layout and instrumentation sites circled and viewed from above (top) and from the side (bottom)

Table 1 Instrumentation details

Data collection method	Collection time interval	Accuracy	Resolution	Number
MPBX	1 min to 24 hr	± 2%	0.254 mm	18
HID-cell	1 min to 8 hr	± 10 ppm	0.1 με	6
Wall-wall convergence	8–12 weeks	± 5 mm	1 mm	15 stations
Floor heave measurement	6 months	± 30 mm	1 mm	15 stations
Damage mapping	10 days to 3 weeks	n/a	n/a	13 sections

3.2 Damage mapping

Damage mapping was completed on a regular basis during the project. Five-metre-wide damage mapping sections were measured and marked on the walls underground with vertical white numbered lines (Figure 5). These lines corresponded to the floor heave mapping locations and the convergence monitoring stations. Photographic records were kept and were very useful for back-analysis and quality control.

(a) (b)

Figure 5 Damage mapping of wall (a) and floor (b)

Crack painting and coloured numbering of major cracks were used to help track new damages as they occurred. Full, complete sets of records were taken regarding the state of the opening, shotcrete damage, rock damage, falls, chips, dust, water and corrosion, bolt and mesh damage, floor heave measurement, etc.

To the greatest extent possible, damage mapping was completed approximately every 2–3 weeks throughout the project and was always completed by the same person. The interval varied depending on time availability, mine area closures, etc. It was clear which entries were changing the most quickly and as such these received greater attention. Damage mapping was also completed before and/or after notable events that were expected to impact entry condition such as nearby production blasting, reinforcement activities, larger seismic events, pre-planned breaks (summer holiday, for example), etc. The cumulative mapping occasions are shown in.

The damage mapping was used to create an ECR system, a calibrated and site-specific system for monitoring and tracking different types of damage occurring in the crosscuts. The system was created in conjunction with the extensometer and stress measurements, all of which served to better understand the crosscut behaviour and interpret the damage progression in a way that reflected the actual mechanisms driving it. This system is fully described in Jones & Saiang (2022a, 2022b) and is similar in function to others published (Kaiser et al. 1992; Lawson & Zahl 2012; Duan et al. 2015; Mikula & Gebremedhin 2017).

The ECR is a two-part system that separates ECR ratings into two different rating scales, before and after reinforcement work in an entry, so that the impact of reinforcement methodology can be better reflected in the rating scale. The primary scale (before reinforcement) is 0–7, with 0 being a freshly made opening and 7 being a rockfall of any type. The secondary scale is I-VI, with I being newly supported/rehabilitated, and VI being a rockfall of any type. The system is generally calibrated so that an ECR of 3 on the primary scale occurs at the same time as instrumentation recorded the maximum confining stress (σ_3) and the deformation rate experienced a sudden jump.

4 Differential stress analysis

The collected 3D stress data was analysed using the cell manufacturer's (ESS Geosystems) analysis software, Stress 201i. After inputting the rock parameters, installation details and cell details the software was used to calculate the daily relative (to the beginning of the study period) primary and tertiary compressive stresses (σ_1 and σ_3) measured throughout the study period.

After determination of the relative primary stresses, the results were used to determine the daily differential stresses according to (Equation 1). These stresses varied from day to day depending on which production blasts had occurred the night before, where the blasts were located, what rock type and/or quality the instrument was installed in, and whether or not there were any mine-sequence related activities (such as

opening a new production level or opening a new crosscut). As the crosscuts were instrumented at different points in their lifetime (new development to mined out), this also played a role in some of the results.

$$\sigma_d = (\sigma_1 - \sigma_3) \quad (1)$$

Based on the ECR developed in the monitored profiles, graphs were made that related the observed ECR to the differential stress recorded at the time the ECR was collected. The outcome was a graph that showed what appeared to be a bilinear relationship between the two variables (Figure 6), shown especially in the biotite and leptite profiles of PR4080 and the magnetite and biotite profiles of AL2780. This matches well with the findings of the deformation measurements from the extensometers which showed a crosscut location tended to remain relatively stable for long periods after development until redistributed stresses became high enough to cause increased deformation rates (Jones & Saiang 2022a). The same type of trend was identified in previous extensometer research in the same mining area (Jones et al. 2019).

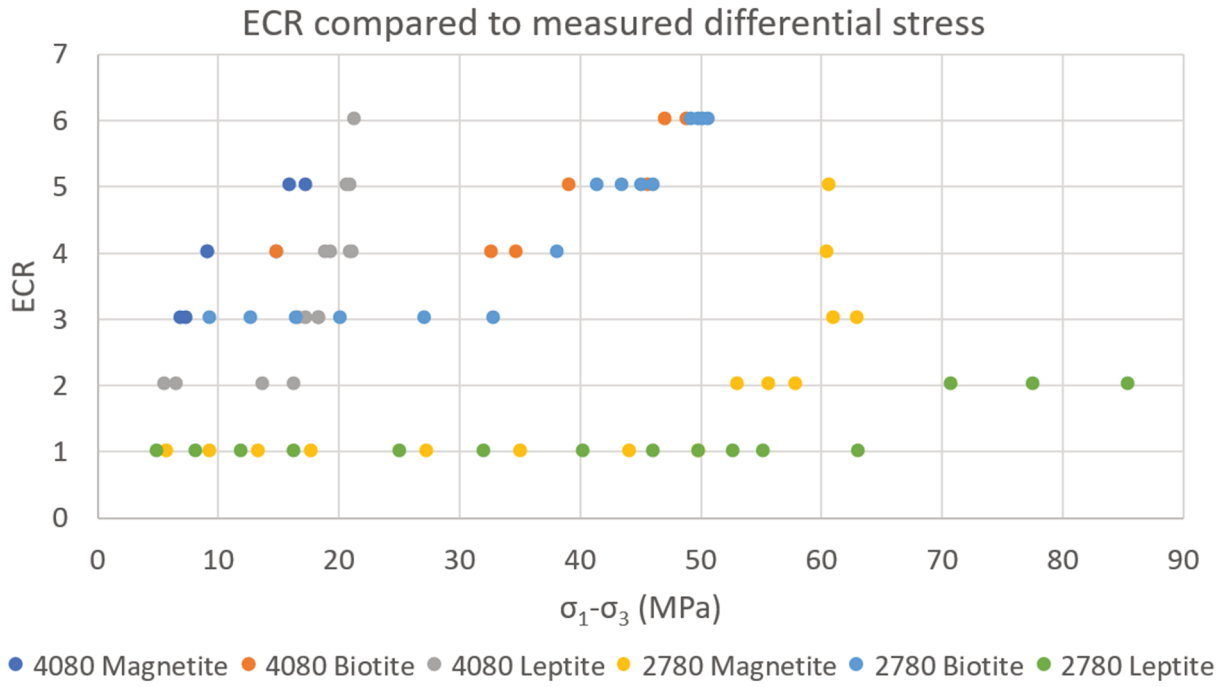

Figure 6 Measured differential stress versus ECR by profile

The remaining profiles on the graph showed that the AL2780 leptite profile never entered the second stage of the bilinear trend before the measurements ended, while in PR4080 the magnetite profile had already entered into the second stage when measurements/observations began. Regardless, with all profiles the range of ECR 2–3 is shown to be the inflection point in ECR/σ_d where small increments of differential stress cause larger increases in the ECR.

While there isn't enough data to proceed further with respect to stage one of damage trend, four of the six profiles have enough data to better understand stage 2. The data was graphed again (Figure 7), this time limiting the data points such that only stage 2 remained. Additionally, differential stress was modified such that for this purpose the σ_d is relative to the date of the maximum confining stress, σ_{3MAX}, which is shown to coincide with the ECR 2–3 inflection point. This new relative differential stress is hereafter termed σ'_d. The purpose here was to determine the ECR rate of change for every incremental increase in σ'_d.

One other modification was made. During the study the PR4080 crosscut had some scaling carried out. This effectively altered the ECR and moved it from a primary ECR (before scaling) to a secondary ECR (after scaling). In addition to the shift in ECR scales, the location also sat without any support other than shotcrete for over three months due to delays from the mine. This led to a much faster rate of degradation that was typical. The data points that were related to this time period were omitted for consistency.

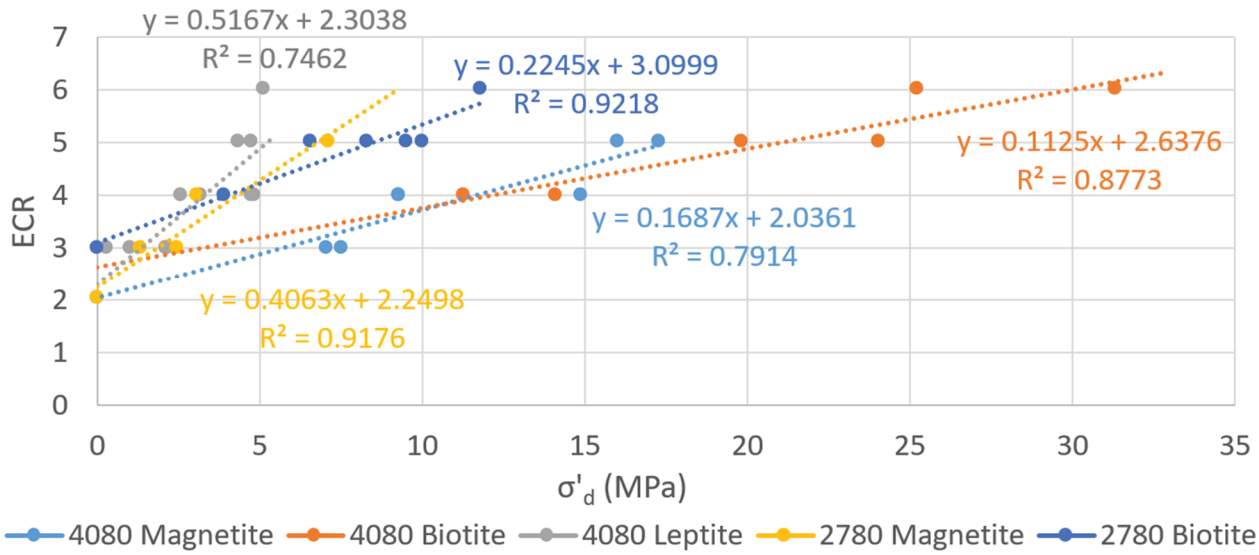

Figure 7 Differential stress and with respect to ECR, stage 2 only

As mentioned, linear relationships between the ECR and the differential stress are apparent in the data and represent the behaviour of the study sites after σ_{3MAX} has occurred or roughly when ECR = 3. The slope of these lines indicates how the opening condition can then be expected to change with respect to induced stress changes once the bilinear trend's stage 2 inflection point has been reached. The general form of the equation relating the two parts of the ECR is as follows in Equations 2 and 3.

$$ECR = ECR_{1MAX} + ECR' \tag{2}$$

where:

ECR_{1MAX} = highest ECR value at prior to the bilinear ECR inflection point for any damage profile.

ECR' = ECR increase following the inflection point for the same damage profile.

and

$$ECR' = K\sigma'_d \tag{3}$$

where:

K = slope of the line (rate of change) relating ECR to σ'_d.

σ'_d = differential stress change relative to σ_{3MAX}.

As the differential stress for each location is specific to that location, the intercept is unnecessary.

The ECR rate of change, *K*, varies greatly between the different damage profiles. To help better understand and define *K* one must look at it with respect to the quality of the rock mass in each location. The damage in a location is highly affected by the condition of the rock due to jointing, fracturing, alterations, and structural deficiencies, and these issues need to be taken into consideration. GSI is used for this purpose based on data from the geologic mapping conducted when the crosscuts were developed.

The mapped GSI and slopes, *K* (Figure 7), are placed together in Table 2, though without the magnetite profile in PR4080. This profile did not have a GSI value recorded and so can't be included in the analysis. The biotite profile for crosscut 2780 had multiple GSI readings taken and so an average was used.

Table 2 GSI and trendline slopes for the ECR' versus differential stress relationship for stage 1 crosscuts. Slopes of the stage 1 crosscuts are also included for comparison (red)

Profile	GSI	K
Leptite 4080	45	0.5167
Biotite 4080	30	0.1125
Magnetite 2780	40	0.4063
Biotite 2780	(45 + 25)/2 = 35	0.2245
Leptite 2780	65	0.0141

These data points are graphed, and another linear relationship is developed allowing prediction of *K* for stage 2 damage dependent upon GSI (Figure 8). This shows the clear relationship between GSI and *K* for stage 2 ECR values and how very different *K* is for stage 1 ECR values. The stage 1 data point, with a GSI of 65, clearly does not belong in the same cluster and is not part of the stage 2 trend.

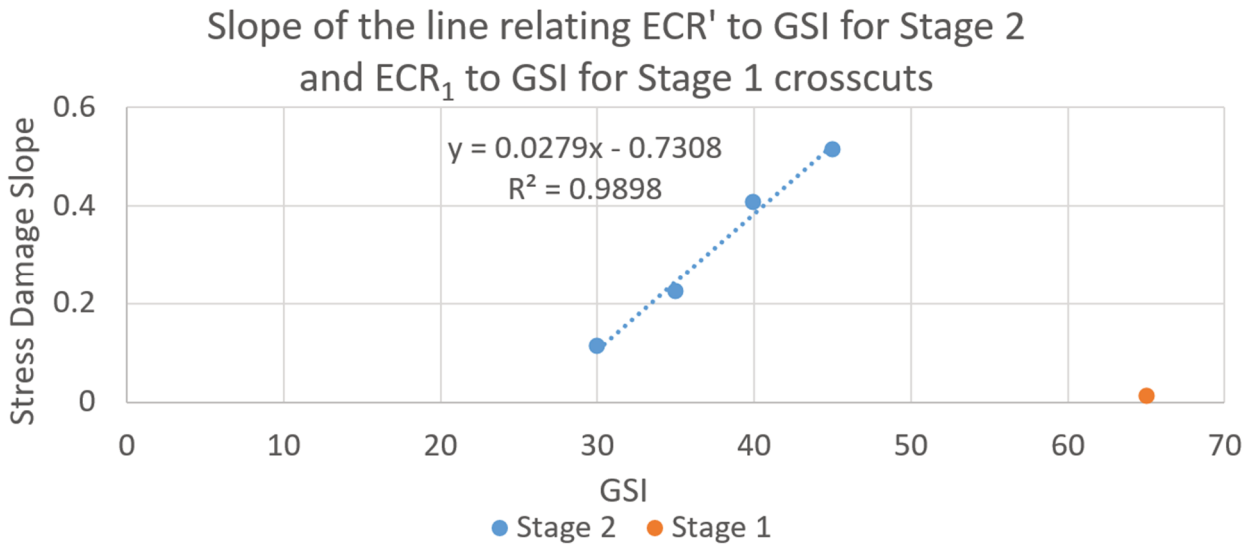

Figure 8 K/GSI relationship

Based on Figure 8 an equation for *K* can be written as in Equation 4, which is the linear trendline for relating the stress damage slope to the GSI. This is roughly how quickly an opening can be expected to degrade under certain stress and rock conditions:

$$K = 0.0279(GSI) - 0.7308 \quad (4)$$

Substituting Equation 4 into Equation 3 gives:

$$ECR' = (0.0279(GSI) - 0.7308)\sigma'_d \quad (5)$$

From Equation 5 the following chart can be built to help predict what damage condition might be expected in an opening compared with a desired reference point in the lifecycle of that opening. When the entire range of GSI possibilities is built together, a single graph is developed that allows the user to view the full relationships (Figure 9).

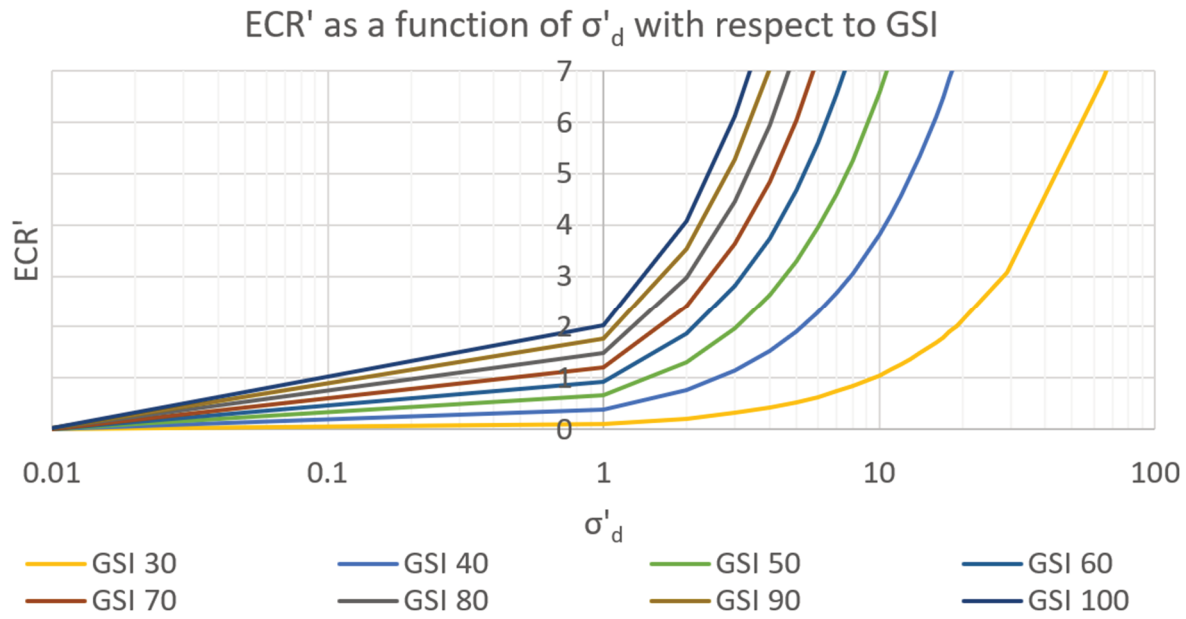

Figure 9 Increase in ECR' following ECR_{1MAX} depending on the changes in stress and GSI value of the rock

5 Discussion

This work can be used in several ways. Most simply, the equations can be used in conjunction with a calibrated numerical model to predict the ECR in each location based on modelled stresses and initial observed damages. If ECR can be predicted, then it can be used to identify ahead of time under which stage of the mining sequence reinforcement may be necessary depending on site-specific data. A rock mechanics engineer can look at the ECR and GSI in a development drift and make a prediction of when mining on the level above will force the development drift to be reinforced.

The damage relationship chart shown in Figure 9 relies on simple relationships between measured data considered to be accurate and a great deal of (admittedly subjective) observational data regarding entry conditions. However subjective the ECR values may ultimately be, the ECR system itself is a validated system that is based upon many different damage profiles in many different conditions, and it is calibrated along with the measured stress data (Jones & Saiang 2022a, 2022b).

An interesting point can be seen with respect to Figure 9. After the rock mass has reached its ECR inflection and entered stage two, a rock with a perfect GSI of 100 will fail very, very quickly, with only a small change in differential stress causing rockfall. This matches well with traditional Mohr–Coulomb theory. The rock has reached the maximum shear stress that is required for the rock to fail. Additionally, a poor-quality rock mass which is capable of holding together some of the fabric of the interlocking pieces is able to move, slide and deform while differential stresses increase, leading to a much greater change necessary to cause rockfall. These field results therefore reflect a classic Mohr–Coulomb material behaviour that exists throughout the spectrum of the different materials found underground.

This method does have some limitations though as it is currently limited by the fact that it is only applicable to the second stage of the trend. The best descriptor of the inflection point is σ_{3MAX} from a modelling point of view, and ECR 2–3 from a damage mapping point of view.

Also, when using this graph some assumptions must be made and some boundary conditions must be set. As a novel tool for predicting entry damage, it is still in its infancy. Its current form includes a low number of data points, gathered from a single mine and from a limited range of GSI values. Even though the geologies and rock properties are varied, they do not represent all geologies. These are standard limitations of empirical data.

6 Conclusion

Empirical observations have always helped us to better understand how the environment around us works. Observations coupled with high-quality measurements are a way to bring a greater level of certainty to our observations and allow us to quantify forces we would be otherwise unable to observe. This paper illustrates a method for taking observations of entry quality, coupling them with quantifiable data in order to validate and support them, and using some standard rock-mechanical principals in order to develop tools capable of informing decisions about rock support.

While site-specific, it is fully reasonable that such a method could be applied at other mining sites and in other conditions. That is one of the strengths of empirical observation – it is highly adaptable and many of the ideas and principals are transferrable, if only the proper alterations can be made to reflect a new site's situation.

This method for entry condition prediction can be used with both numerical modelling – for estimating future conditions based on modelled stresses and information about the rock quality, or based on site damage mapping and periodic inspections, as a tool to properly respond to observed damage. In the first case it offers the potential to adjust primary rock support to better address the needs of a particular location, and in the second it offers an opportunity to prioritise reinforcement activities. In both cases it provides an opportunity to reduce the risk to health, safety and operation.

Acknowledgement

This paper is an outcome of project number 406, Design Methods for Variable Stress, Variable-Geology Environments, of the Swedish Rock Engineering Research Foundation (Stiftelsen Bergteknisk Forskning), Luossavaara Kiirunavaara AB, and the Luleå University of Technology. Special thanks to these organisations for their support.

References

Bergman, S, Kübler, L & Martinsson, O 2001, 'Description of regional geological and geophysical maps of northern Norrbotten county (east of the Caledonian orogen)', Sveriges Geologiska Undersökning, Östervåla.

Duan, W, Wesseloo, J & Potvin, Y 2015, 'Evaluation of the adjusted rockburst damage potential method for dynamic ground support selection in extreme rockburst conditions', in Y Potvin (ed.), *Design Methods 2015: Proceedings of the International Seminar on Design Methods in Underground Mining*, Australian Centre for Geomechanics, Perth, pp. 399–418, https://doi.org/10.36487/ACG_rep/1511_24_Duan

Feng, X, Zhao, J, Wang, Z, Yang, C, Han, Q & Zheng, Z 2021, 'Effects of high differential stress and mineral properties on deformation and failure mechanism of hard rocks', *Canadian Geotechnical Journal*, vol. 58, no. 3, pp. 411–426.

Jones, T, Nordlund, E & Wettainen, T 2019, 'Mining-induced deformation in the Malmberget mine', *Rock Mechanics and Rock Engineering*, vol. 52, pp. 1903–1916, https://doi.org/10.1007/s00603–018–1716–6.

Jones, T & Saiang, D 2022a, *Report 209: Design Methods for Variable-Stress, Variable-Geology Environments*, Stiftelsen Bergteknisk Forskning, Stockholm.

Jones, T & Saiang, D 2022b, 'Empirical damage prediction in sublevel cave crosscuts at the Malmberget mine', in: Y Potvin (ed.), *Caving 2022: Proceedings of the Fifth International Conference on Block and Sublevel Caving*, Australian Centre for Geomechanics, Perth, pp. 1001–1012.

Kaiser, PK, Tannant, DD, McCreath, DR & Jesenak, P 1992, 'Rockburst damage assessment procedure', in PK Kaiser & DR McCreath (eds), *Rock Support in Mining and Underground Construction*, A.A. Balkema, Rotterdam.

Lawson, H & Zahl, E, 2012, 'Ground Condition Mapping: A Case Study', paper presented at SME Annual Meeting and Exhibit, Seattle, 19–22 February, Preprint number 12–122 6.

Mikula, P & Gebremedhin, B 2017, 'Empirical selection of ground support for dynamic conditions using charting of support performance at Hamlet mine', in J Wesseloo (ed.), *Deep Mining 2017: Proceedings of the Eighth International Conference on Deep and High Stress Mining*, Australian Centre for Geomechanics, Perth, pp. 625–636, https://doi.org/10.36487 /ACG_rep/1704_42_Mikula